View metadata, citation and similar papers at core.ac.uk
brought to you by CORE
provided by Universidade do Minho: RepositoriUM

Appl. Phys. A (2016) 122:820
DOI 10.1007/s00339-016-0354-7

Applied Physics A
Materials Science & Processing

Metal alloys, matrix inclusions and manufacturing techniques of Moinhos de Golas collection (North Portugal): a study by micro-EDXRF, SEM–EDS, optical microscopy and X-ray radiography

Joana Loureiro[1] · Elin Figueiredo[2] · Rui J. C. Silva[2] · M. Fátima Araújo[3] · João Fonte[4,5] · Ana M. S. Bettencourt[5]

Received: 20 July 2015 / Accepted: 7 August 2016
© Springer-Verlag Berlin Heidelberg 2016

Abstract A collection of 35 metallic artefacts comprising various typologies, some of which can be attributed to the Bronze Age and others to later periods, were studied to provide detailed information on elemental composition, manufacturing techniques and preservation state. Elemental analysis by micro-EDXRF and SEM–EDS was performed to investigate the use of different alloys and to study the presence of microstructural heterogeneities, as inclusions. X-ray radiography, optical microscopy and SEM–EDS were used to investigate manufacturing techniques and degradation features. Results showed that most of the artefacts were produced in a binary bronze alloy (Cu–Sn) with 10–15 wt% Sn and a low concentration of impurities. Other artefacts were produced in copper or in brass, the latest with varying contents of Zn, Sn and Pb. A variety of inclusions in the metal matrices were also found, some related to specific types of alloys, as $(Cu–Ni)S_2$ in coppers, or ZnS in brasses. Microstructural observations revealed that the majority of the artefacts were subjected to cycles of thermomechanical processing after casting, being evident that among some artefacts different parts were subjected to distinct treatments. The radiographic images revealed structural heterogeneities related to local corrosion processes and fissures that seem to have developed in wear-tension zones, as in the handle of some daggers. Radiographic images were also useful to detect the use of different materials in one particular brass artefact, revealing the presence of a possible Cu–Sn solder.

✉ Elin Figueiredo
emf12055@campus.fct.unl.pt

[1] Departamento de Conservação e Restauro, Faculdade de Ciências e Tecnologia, Universidade NOVA de Lisboa, Quinta da Torre, 2829-516 Caparica, Portugal

[2] Centro de Investigação em Materiais (CENIMAT/I3N), Departamento de Ciência dos Materiais, Faculdade de Ciências e Tecnologia, Universidade NOVA de Lisboa, Quinta da Torre, 2829-516 Caparica, Portugal

[3] Centro de Ciências e Tecnologias Nucleares (C2TN), Instituto Superior Técnico, Universidade de Lisboa, Estrada Nacional 10, ao km 139,7, 2695-066 Bobadela LRS, Portugal

[4] Instituto de Ciencias del Patrimonio (Incipit), Consejo Superior de Investigaciones Cientificas (CSIC), Santiago de Compostela, Spain

[5] Laboratório de Paisagens, Património e Território (Lab2PT/UM), Departamento de História, Universidade do Minho, Campus de Gualtar, 4710-057 Braga, Portugal

1 Introduction

The study of ancient metallic artefacts involving elemental, structural and microstructural characterizations can be very relevant to investigate the type of metals and alloys used to produce them, as well as the manufacturing processes involved in the shaping of different objects. Understanding the materials and technologies employed in certain regions or periods can also help in tracing ancient contacts among different cultures whenever exchange of artefacts, raw materials or technologies happened [1, 2]. Additionally, by studying the materials and structural features important information can be provided on the preservation state of artefacts and thus be useful to create adequate guidelines for the handling and future storage of the artefacts.

In 2003, an interesting archaeological site was discovered in northern Portugal, Moinhos de Golas (MG) (Montalegre, Vila Real). It occupies a slightly elevated hill overlooking the Assureira stream and has large-size granitic outcrops that naturally emphasize the site [3]. No archaeological excavations were made, but a collection of

35 metallic artefacts were recovered by a local resident. All artefacts were incorporated in the Archaeological Museum of Braga (Museu de Arqueologia D. Diogo de Sousa). In 2013, a team of archaeologists visited the site to verify the location of the metal finds and collected some pottery sherds with characteristics of the regional Late Bronze Age (LBA) (twelfth to seventh/sixth centuries BC) [3].

The metallic collection, collected in different places of the hill [3], shows artefacts of various typologies, as well as fragments of objects or semi-finished objects. It is composed by 3 weapons (daggers of different sizes and shapes but attributed to Porto de Mós type), 5 ornaments (one button, two possible pendants or hair pins, one nail and a small capsule), 1 tool (tranchet), as well as others of difficult classification, which include 17 rings (which can be grouped into 3 different sizes), 8 bars of different sizes and shapes (some of which can belong to undetermined broken objects as one composed by one wire and two rings, and others to semi-finished objects), and one small thin-folded sheet (Fig. 1).

Typologically, the daggers and the tranchet can be attributed to the LBA, and similar objects have been found in the Portuguese territory. Buttons similar to the one found in MG are also known in LBA or Early Iron Age contexts of western Iberian Peninsula [4, 5]. A capsule similar to the MG one was found in a Megalithic grave in the central region of Portugal and was interpreted as a result of a LBA reuse of the grave [6]. On the other hand, the broken objects, as the majority of bars, are of difficult chronological and cultural classification. The rings cannot be attributed to any particular chronological context either, since they can be found from LBA to much later periods.

A preliminary study of the collection pointed out the presence of artefacts made of copper, bronze and brass [7]. This could suggest the presence of artefacts from different metallurgical origins and/or from various chronological periods, especially due to the presence of brasses. Brasses are generally attributed to Roman or later productions, being that earlier brasses have only been found in eastern Iberia in the context of Mediterranean influence (as Phoenician/Punic), from the sixth to the third centuries BC [8].

In the Portuguese territory, and during LBA, most artefacts were produced in a binary bronze alloy, with a low impurity pattern. By this time, only few artefacts were produced in leaded bronze or unalloyed copper [9, 10]. However, recent studies, most from the southern Portuguese territory, have pointed out the possibility of differentiating these bronzes from those with Mediterranean influences [attributed to the later Iron Age (IA)] by the tin content and impurity pattern [11–15]. Generally, during LBA, the Sn content of the objects shows a normal distribution between $\sim$8 and 15 wt% Sn, and the alloy has a low impurity pattern, namely $<$0.05 wt% Fe, $<$0.5 wt% As and $<$0.5 wt% Pb. Later bronzes generally show more dispersed and lower Sn contents, $<$10 wt% Sn, higher Pb and As contents, and most notably, have an Fe content frequently $>$0.05 wt%. While the lower and more disperse Sn contents can be a result of intentional fabrication of alloys with diverse compositions, it can also be attributed

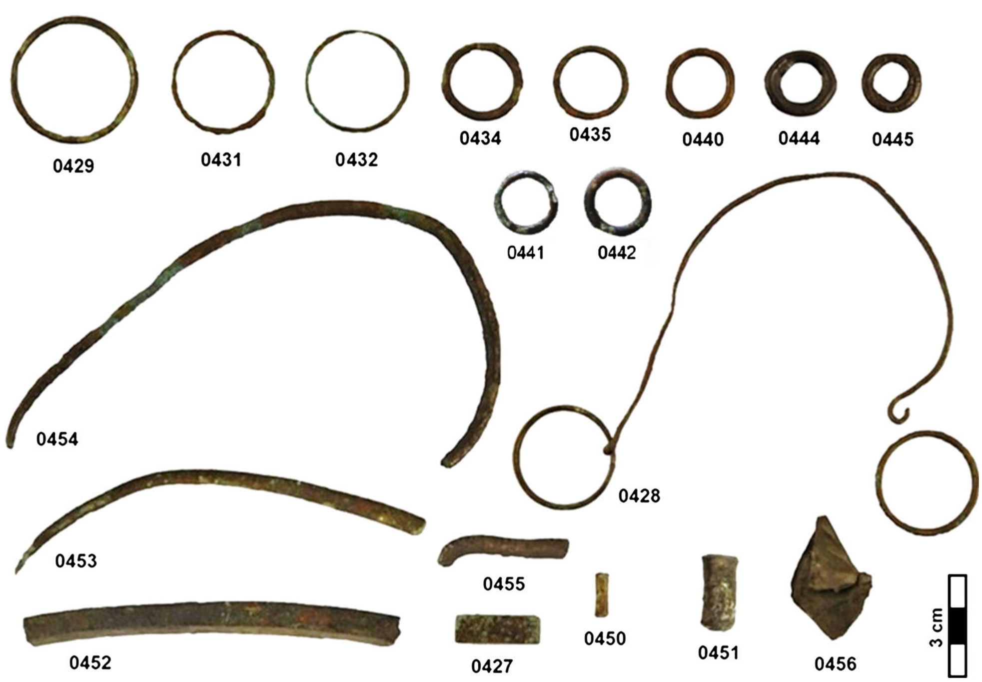

Fig. 1 Part of the studied Moinhos de Golas collection, mostly *rings* and *bars*

to metal recycling and preferential Sn loss. Higher Pb and As contents could also be due to the use of new type of alloys, or to the use of other sources in addition to the recycling factor. On the other hand, the Fe content has been associated with a change in smelting conditions that occurred during Phoenician colonization (during early first millennium BC), which allowed the incorporation of iron into the alloy by smelting in more reducing atmosphere and higher temperatures [16]. Scarce studies on the composition of inclusions in the metal matrices have been made [11]. It has been shown that Cu–S inclusions are frequent in copper and bronzes from Bronze Age onwards and that bronzes can also show Cu–S–Fe, Sn–O and Pb inclusions. In bronzes with Mediterranean influences, the type of inclusions seems to be similar to the ones of the earlier period.

In the present work, a detailed characterization of the MG metal collection is aimed, focusing on the composition of metal matrices and inclusions, and on the structure and microstructure of the artefacts. This will be relevant to provide information on the metallurgy of those artefacts attributed to LBA, and to characterize the metallurgical production of those artefacts of difficult chronological contextualization. This can provide information about differences between bronze artefacts, and relate some of them to productions of more Mediterranean influence.

The structural and microstructural studies can provide details on the conservation state of the objects, of relevance for museum conservation strategies, and reveal the manufacturing procedures used to shape specific parts of objects.

The Moinhos de Golas site is located in a region with proven occupations from the Bronze Age, Iron Age, Roman [17] as well as Medieval, enabling a deposition or loss of artefacts at different moments at the site. One of the most important natural richnesses of the region, and of ancient interest, are rich tin ore deposits (cassiterite) [5] that could have been exploited since the Bronze Age, and during different periods of time, supporting a regular presence and passage of people in the area.

The presence of brasses in the collection is very interesting. Until present, very few studies have been made on brasses of the Iberian territory, including Roman ones. The presence of brasses is known in eastern Iberian regions from at least the sixth century BC in colonial contexts, or in Iron Age contexts of the fourth to third centuries BC [8]. These few objects have shown Zn contents in the range of 8–18 wt% Zn, occasionally 1–2 wt% Sn and up to 5 wt% Pb. They have been explained as importations from the eastern Mediterranean. In the eastern Mediterranean, the earliest known brasses are two rings from the thirteen century BC, found in Iraq, that have 15 and 12 wt% Zn, 0.5 and 6 wt% Sn, and 5 and 3 wt% Pb, respectively. In the eastern Iberian Peninsula other objects with lower and variable contents of Zn have been explained as a result of recycling, as by mixing exogenous brasses that circulated at the time with other metals [8].

While the first brass productions resulted in alloys of variable contents of Zn (due to the high volatility of Zn that could make the brass production problematic), from the first century BC onwards, with the cementation process, a higher control in the alloy fabrication was possible [18–20]. Due to the cementation process, the Romans began mass production of brass with relatively high Zn contents, around 18–20 wt% Zn [21, 22]. During Roman times, copper alloys were also known to be frequently recycled, and new alloys with specific characteristics could have been made by mixing different metals in a deliberate way [21].

For the present work, a combination of analytical and examination techniques was used to provide complementary, detailed and relevant archaeometallurgical information, following a minimally invasive analytical procedure. Digital X-ray radiography was used to investigate structural heterogeneities that could be related to specific manufacturing techniques or to the alteration and corrosion of metal. Elemental analysis by micro-X-ray fluorescence (micro-EDXRF) was performed on small cleaned surfaces of the artefacts (avoiding altered corrosion layers) to attain the composition of the alloys. The same cleaned areas were used for optical microscopy (OM) observations, for the identification of different phases, inclusions and other microstructural features related to specific processing sequences. Scanning electron microscopy with energy dispersive spectroscopy (SEM–EDS) was used for the characterization of the inclusions on selected artefacts and to investigate a possible solder vestige in a brass capsule.

2 Experimental

2.1 X-ray radiography

Radiographic images were obtained with a digital X-ray system, ArtXRay, SEZ Series, manufactured by NTB GmbH (Dickel, Germany). The parameters used were a voltage of 130 kV and current intensity of 3.7 mA (480 W), which consists of the maximum power capacity of the equipment. This was adequate for the structural study of most artefacts, especially for those of thinner or near-flat cross sections. The set-up of the analysis involved a focus–detector distance of 1.36 m, with the artefacts positioned within a distance of circa 14 cm from the detector. The image processing involved the iX/Pect software, which allows for the regulation of the grey-level scale. This allowed for a processing of the radiographic images, by being able to fit the grey-level scale suppressing low levels which constituted background artefacts in the original images and also changing the linear variation of the grey-level intensities to be able to put small variations in the X-rays transmittance into evidence.

2.2 Micro-EDXRF

Micro-EDXRF analyses were performed in most metal artefacts in a small area free from the superficial corrosion layers. Only two artefacts, two rings, were not cleaned due to their fragile preservation state being the results of the analyses only considered semi-quantitatively. The prepared areas were metallographically prepared by manual polishing with several diamond suspensions (6 µm until ¼ µm) in a cotton swab, allowing for the removal of the superficial corrosion layers in a small area (<5 mm^2).

The analyses were performed in an ArtTAX Pro spectrometer which comprises: a low-power X-ray tube with a Mo anode; a set of polycapillary lens that generate a microspot of ~70 µm in diameter of primary radiation; an integrated CCD camera and three beam-crossing diodes which provide the control over the exact position on the sample to be analysed; and a silicon drift electro-thermally cooled detector with a resolution of 160 eV at Mn–Kα [23]. The artefacts were analysed in 3 different spots in the prepared areas using 40 kV, 0.5 mA and 100 s of tube voltage, current intensity and live time, respectively.

Quantitative analysis was made using Winaxil software that uses fundamental parameter method and experimental calibration factors that were calculated with certified reference materials: Phosphor Bronze 551 Spectrographic Standard from British Chemical Standards (BCS) for the copper and bronze alloy and Free-Cutting Brass 1103 from National Bureau of Standards (NBS) for the brass alloys. The determination of the accuracy of the analytical procedure was accomplished by the analysis and quantification of other certified reference materials, Phosphor Bronze 552 from BCS and Free-Cutting Brass 1104 from NBS for the brass alloys, using the same experimental conditions (Table 1). Experimental relative errors can be considered lower than 5 % for major elements and lower than 15 % for minor elements, while quantification limits for minor elements detected are 0.50 wt% Sn, 0.20 wt% Zn, 0.10 wt% Pb, As and Ni, and 0.05 wt% Fe.

2.3 SEM–EDS

The SEM analyses were performed in a Zeiss equipment, model DSM 962 which has backscattered electrons (BSE) and secondary electrons (SE) imaging modes and an energy dispersive spectrometer (EDS) from Oxford Instruments model INCAx-sight with an ultra-thin window, able to detect low atomic number elements as oxygen and carbon. The analyses were made with a working distance of 25 mm, an acceleration voltage of 20 kV, a filament current of ~3 A and an emission current of 70 µm. Elemental semi-quantifications were made using ZAF correction factors. The analyses were performed without any superficial conductive coating (such as carbon or gold) following an experimental procedure previously developed for archaeological metals [24].

2.4 Optical microscopy

The OM observations were conducted in a motorized Leica DMI5000M microscope. This microscope is coupled to a computer with the LAS version 2.6 software which allows for the use of multifocus functionality, essential to the observation of non-flat surfaces as the ones resulting of the local metallographic manual preparation [25]. This feature added to the characteristic of inverted lenses allows the examination of small prepared areas of large-size artefacts without the need of sampling. The initial microstructure examinations were made in bright field (BF) and under polarized light (Pol) with the surface in as-polished state. After these observations, the surfaces were etched with an

Table 1 Relative errors associated with the micro-EDXRF quantitative analyses by the analysis of two certified reference materials (average ± one standard deviation for 3 spot analyses)

	Cu	Sn	Pb	Fe	Ni
BCS SS552					
Certified (wt%)	87.7	9.78	0.63	0.10	0.56
Obtained (wt%)	88.6 ± 0.2	9.70 ± 0.10	0.61 ± 0.09	0.11 ± 0.02	0.56 ± 0.03
Relative error	1 %	−0.8 %	-3 %	13 %	0.6 %

	Cu	Sn	Pb	Fe	Ni	Zn
NBS 1112						
Certified (wt%)	61.33	0.43	2.77	0.088	0.07	35.31
Obtained (wt%)	61.6 ± 0.2	0.45 ± 0.01	2.67 ± 0.07	0.09 ± 0.00	0.08 ± 0.01	35.1 ± 0.2
Relative error	−0.5 %	4 %	−3 %	−0.1 %	11 %	−0.6 %

aqueous ferric chloride solution (prepared according to: 120 ml of deionized water, H_2O; 30 ml of concentrated hydrochloric acid, HCl; and 10 g of ferric chloride, $FeCl_3$ [26]) in order to reveal microstructural features such as grain boundaries, annealing twins and slip bands among the grains, which are important features to characterize specific thermomechanical treatments which have been performed to shape the artefacts.

3 Results and discussion

3.1 Structural heterogeneities by digital X-ray radiography

Radiographic images were digitally processed so that structural and material heterogeneities were put into evidence. Through digital treatment, the linear relationship between grey-level intensity and higher thicknesses and/or materials with higher attenuation coefficients could be manipulated, putting heterogeneities implicit in small grey-level ranges into evidence. This resulted in a clearer observation of some relevant structural features. In the daggers, the areas with corrosion and areas with thin fissures were put into evidence. In Fig. 2, different corrosion behaviours are shown, as the regular external corrosion layer on both daggers, evidenced as a dark outline in the processed radiographs, and some localized and deeper corrosion regions in dagger 0423, corresponding to areas of stronger corrosion and some loss of material (pictured as heterogeneities of semicircular shape along the blade). In both daggers, there is a fissure on the top of the handle that appears to be located in the area where the beginning of a hilt was originally positioned, suggesting that this area could have been subjected to some pressure/tension leading to the development of fissures. A fissure is also present further down the blade of dagger 0425, and in the dagger 0423 some thin fissures seem to irradiate from the hole at the top where a rivet would have been placed, suggesting tensions at this grip area as well.

Additionally, at the top of the dagger 0425 three small areas of higher X-ray transmission were put into evidence. Micro-EDXRF analyses made at the corresponding areas of these circles, over the corrosion products, revealed no differences to the spectra obtained on various points on the rest of the surface of the object. Observations under stereomicroscope were not conclusive either. However, they suggested a slightly lower thickness in these areas.

The morphological structures of the thin sheet 0456 and the nail 0447 were better revealed with the radiograph images. In Fig. 3, the original and a digitally treated radiograph of each one of these artefacts are shown. The folded part of the sheet becomes evident, as well as other bending actions to which the sheet was submitted, resulting in fragilized areas/lines of higher X-ray transmission. In the treated radiograph of the nail, the hollow area inside the pin head and the attaching region of the pin can be clearly observed.

Through the radiographic investigation, it was also possible to detect the presence of different materials in one artefact, the metallic capsule 0457 (Fig. 4a). Its

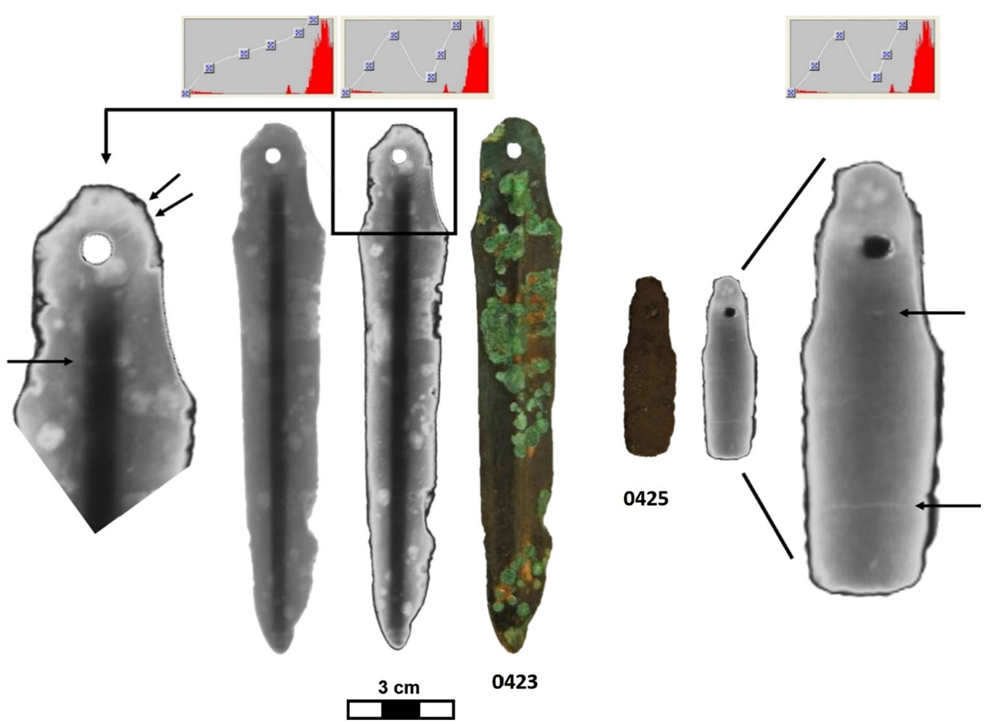

Fig. 2 X-ray digital radiographic images of the daggers 0423 and 0425 with the position of some thin fissures depicted by *arrows* (*greyscale* has been altered to evidence structural heterogeneities)

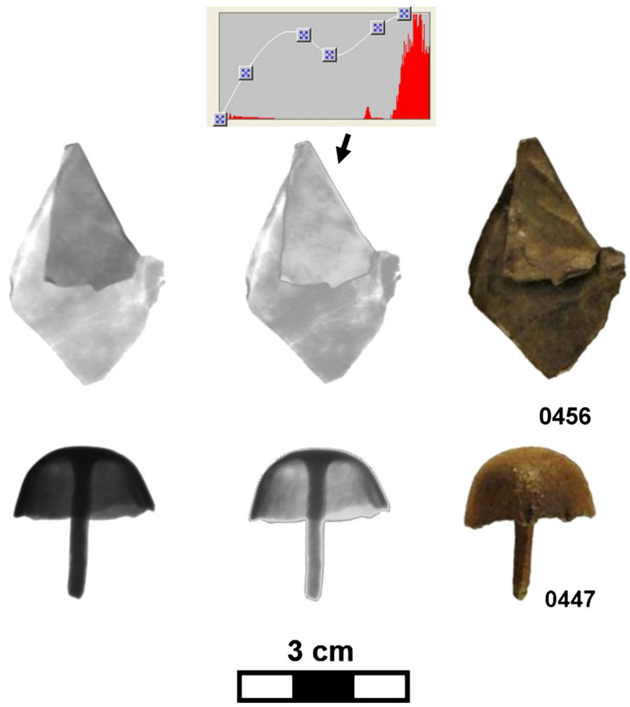

Fig. 3 X-ray digital radiographic images of the thin-folded sheet 0456 and the nail 0447 (*greyscale* has been altered to evidence structural heterogeneities at the middle image)

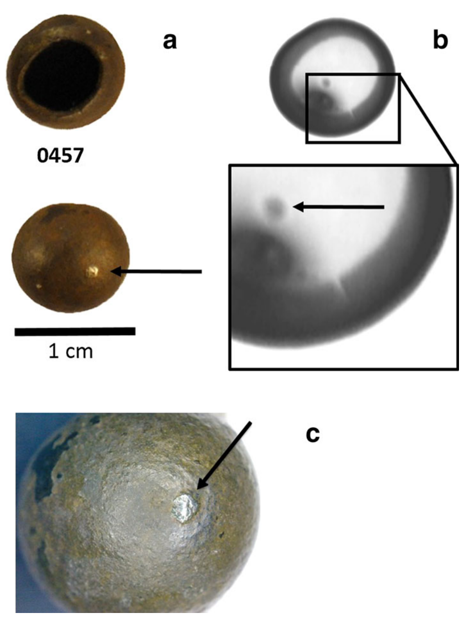

Fig. 4 Images of the capsule 0457: **a** photographs in different positions; **b** X-ray digital radiography; **c** stereomicroscope image of the surface. A small material of a different composition is depicted in the images (visible by eye after local cleaning)

radiographic image shows a small dark spot (Fig. 4b) near a larger dark area which corresponds to some earth deposits on the inside of the capsule. Visual inspection allowed to identify a small-size adherent material present in the outer surface of the capsule, which was locally cleaned from the superficial corrosion layers and revealed a silvery colour, suggesting a material of a different composition from the base metal (Fig. 4c). It has to be highlighted that this material had not been detected previously to the radiographic image due to the presence of a homogeneous corrosion layer, and its discovery allowed for its later characterization.

3.2 Composition of metals and inclusions by micro-EDXRF and SEM–EDS

The results of the micro-EDXRF analysis (Table 2) show that most of the artefacts are made by a binary bronze alloy (Cu–Sn alloy) and six objects are made in copper (3 rings, 2 bent bars and the bent sheet), three of which with low amounts of Sn ($\sim$1 wt% Sn). The remaining three objects (a capsule and two rings) are made out of a copper alloy with zinc (contents 9–19 wt% Zn), thus classified as brasses. Among these 3 objects, the two rings also show variable amounts of other elements, namely Sn ($\sim$3–4 wt%) and Pb (one with $\sim$7 wt%), which could make them be designated as gunmetal and leaded gunmetal alloys in certain metallurgical contexts.

The results of the identification of inclusions by SEM–EDS in selected artefacts of each type of metal are summarized in Table 3, and some BSE images with the identification of some inclusions are shown in Fig. 5. Generally, it could be observed that a relatively large variety of inclusions were found and that some of them are related to a specific type of metal. The Cu_2S inclusions are present in the bronzes, and in the coppers this type of inclusion shows the presence of some Ni content. A complex oxide inclusion with S and Fe, represented by Cu–Sn–S–Fe–O, was detected only in the bronzes. This type of inclusion can be related to inclusions interpreted as Cu–S–Fe in past works [11]. The coppers also show SnO_2 inclusions and in one of them Bi was also found. All the brasses show Pb inclusions or Pb with minor amounts of Bi (in the ring 0442 the $\sim$7 wt% Pb can be understood as an alloy element; Pb and Bi are immiscible elements in copper), and one ring and the capsule have ZnS inclusions while the other ring has Cu_2S inclusions. The brass capsule also shows Bi inclusions.

In the major group of artefacts, the bronzes, the tin contents are mainly between 10 and 15 wt% (the exceptions are one bar with $\sim$5 % and one ring with $\sim$8 % Sn) (Fig. 6). This alloy composition and the low content of impurities, namely Fe (<0.05 wt%) and Pb (<0.5 wt%), can relate these objects to the bronze composition from various Late Bronze Age collections from the Portuguese territory [10, 12, 15, 27]. The type of inclusions identified

Table 2 Micro-EDXRF results of bronzes, coppers and brasses from Moinhos de Golas collection (values in wt% and normalized)

Artefact	References	Cu	Sn	Pb	As	Fe	Zn
Bronzes							
Dagger	0423	86.7 ± 1.1	12.8 ± 1.2	0.3 ± 0.1	<0.10	<0.05	n.d.
Dagger	0424	86.1 ± 0.4	13.3 ± 0.5	0.4 ± 0.0	<0.10	<0.05	n.d.
Dagger	0425	84.4 ± 1.1	15.3 ± 1.1	0.2 ± 0.0	<0.10	<0.05	n.d.
Tranchet	0425	85.1 ± 0.3	14.9 ± 0.3	n.d.	<0.10	<0.05	n.d.
Bar	0427	84.1 ± 3.3	13.8 ± 0.3	n.d.	0.09 ± 0.01	<0.05	n.d.
Copper wire with 2 bronze rings	0428-ring1	86.5 ± 0.3	13.2 ± 0.3	n.d.	0.19 ± 0.01	<0.05	n.d.
	0428-ring2	86.3 ± 0.2	13.5 ± 0.1	n.d.	0.12 ± 0.01	<0.05	n.d.
Ring	0429	87.4 ± 0.4	12.7 ± 0.2	n.d.	<0.10	<0.05	n.d.
Ring	0430	88.2 ± 0.6	11.8 ± 0.6	n.d.	n.d.	<0.05	n.d.
Ring	0431	86.8 ± 0.1	13.0 ± 0.1	n.d.	<0.10	<0.05	n.d.
Ring	0436	87.8 ± 1.3	12.0 ± 1.2	n.d.	0.11 ± 0.01	<0.05	n.d.
Ring	0438	85.2 ± 0.9	14.6 ± 0.9	n.d.	0.13 ± 0.01	<0.05	n.d.
Ring	0439	85.8 ± 0.6	13.8 ± 0.5	0.2 ± 0.1	<0.10	<0.05	n.d.
Ring	0440	85.3 ± 0.6	14.5 ± 0.6	0.1 ± 0.0	<0.10	<0.05	n.d.
Ring	0443	89.0 ± 1.6	10.6 ± 1.5	0.3 ± 0.1	<0.10	<0.05	n.d.
Ring	0444	85.8 ± 1.0	13.6 ± 1.0	0.3 ± 0.0	0.12 ± 0.01	<0.05	n.d.
Ring	0445	90.7 ± 0.9	8.1 ± 0.8	0.8 ± 0.1	0.21 ± 0.02	<0.05	n.d.
Button	0446	87.7 ± 0.6	12.0 ± 0.7	0.2 ± 0.0	<0.10	<0.05	n.d.
Nail	0447	89.8 ± 0.5	10.0 ± 0.5	0.1 ± 0.1	<0.10	<0.05	n.d.
Pendant	0448	86.4 ± 0.1	13.2 ± 0.1	0.2 ± 0.0	<0.10	<0.05	n.d.
Pendant	0449	88.4 ± 1.5	12.3 ± 1.5	0.1 ± 0.1	<0.10	<0.05	n.d.
Bar	0450	86.9 ± 1.04	13.0 ± 1.1	n.d.	<0.10	<0.05	n.d.
Bar	0451	87.8 ± 0.8	12.0 ± 0.8	n.d.	0.14 ± 0.01	<0.05	n.d.
Bar	0452	87.9 ± 0.7	11.9 ± 0.7	n.d.	0.15 ± 0.01	<0.05	n.d.
Bar	0454	94.7 ± 0.9	4.9 ± 0.9	0.2 ± 0.1	<0.10	<0.05	n.d.
Bar	0455	87.6 ± 0.8	12.1 ± 0.8	0.2 ± 0.1	<0.10	<0.05	n.d.
Coppers							
Copper Wire with 2 bronze rings	0428-wire	99.9 ± 0.1	n.d.	n.d.	<0.10	<0.05	n.d.
Ring	0434	98.4 ± 0.6	1.3 ± 0.6	n.d.	0.10 ± 0.03	0.05 ± 0.08	n.d.
Ring	0435	98.8 ± 0.3	1.2 ± 0.3	n.d.	n.d.	<0.05	n.d.
Ring	0437	99.9 ± 0.0	n.d.	n.d.	<0.10	<0.05	n.d.
Bar	0453	98.4 ± 0.2	1.3 ± 0.3	n.d.	<0.10	<0.05	n.d.
Sheet	0456	99.1 ± 0.1	n.d.	0.1 ± 0.0	0.75 ± 0.02	<0.05	n.d.
Brasses							
Ring	0441	82.0 ± 1.0	2.9 ± 0.1	0.3 ± 0.1	<0.10	0.35 ± 0.01	14.5 ± 1.0
Ring	0442	79.7 ± 3.2	3.5 ± 0.5	7.2 ± 2.8	<0.10	0.28 ± 0.02	9.1 ± 0.7
Capsule	0457	79.0 ± 1.0	n.d.	0.7 ± 0.3	0.79 ± 0.04	0.07 ± 0.01	19.4 ± 0.7

in two bronzes, Cu_2S and Cu–Sn–S–Fe–O, can also be considered as related to bronzes from this period [11].

The copper artefacts show some singularities, namely their type of inclusions. Inclusions of Cu_2S have previously been identified in coppers from Late Bronze Age contexts, but the present ones ($(Cu–Ni)_2S$) show the presence of Ni. EDS analysis made to the alpha copper phase in both coppers showed the presence of <1 wt% Ni in solid solution, which can explain the association of Ni with Cu in this type of inclusion at these artefacts. Inclusions of SnO_2 have previously been found in other Iberian artefacts, but in bronzes. In the present case, these inclusions can partially account for the Sn content detected in the micro-EDXRF analysis. On the other hand, Bi inclusions have not been described until present among Bronze Age copper or bronzes from western Iberia. The presence of these types of

Table 3 Inclusions in metal matrices identified by SEM–EDS analysis

Artefact	References	Inclusions	Metal
Ring	0430	Cu_2S/SnO_2/Cu–Sn–S–Fe–O	Bronze
Ring	0431	Cu_2S/Cu–Sn–S–Fe–O	Bronze
Ring	0434	Bi/$(Cu–Ni)_2S$/SnO_2	Copper
Ring	0435	$(Cu–Ni)_2S$/SnO_2	Copper
Ring	0441	Pb/Cu_2S	Brass
Ring	0442	Pb/ZnS	Brass
Capsule	0457	Bi/Pb(–Bi)/ZnS	Brass

inclusions is possibly related to the type of original ore used to produce the metal. The presence of bismuth has been related to the type/source of the ores used for smelting [28] and can sometimes be associated with other impurities as arsenic, antimony and nickel (e.g. in an enriched Fahlerz-type ore) [29]. To present, it is not possible to point out any specific chronology or cultural context for these coppers. It can only be suggested that they seem to originate from a different metallurgical context than the analysed bronzes, and the 0.05 wt% Fe in one of the artefacts (the ring 0434) can also point out to this direction.

Two copper rings and one bar show small amounts of Sn. In the north of Portugal, a small quantity of Sn was detected in a copper Tartessian belt hook fragment (with 0.8 wt% Sn and 0.11 wt% Fe) within a collection of artefacts with Mediterranean affiliations [30]. Also, it has been demonstrated that by Roman time, and in some regions, copper alloys with 1–5 wt% Sn, and thus with properties similar to pure copper, were largely used to produce wires and sheet-based objects [21]. Taking the presence of one copper sheet and three bars/wires of copper with up to 5 wt% Sn into account, one cannot exclude the possibility

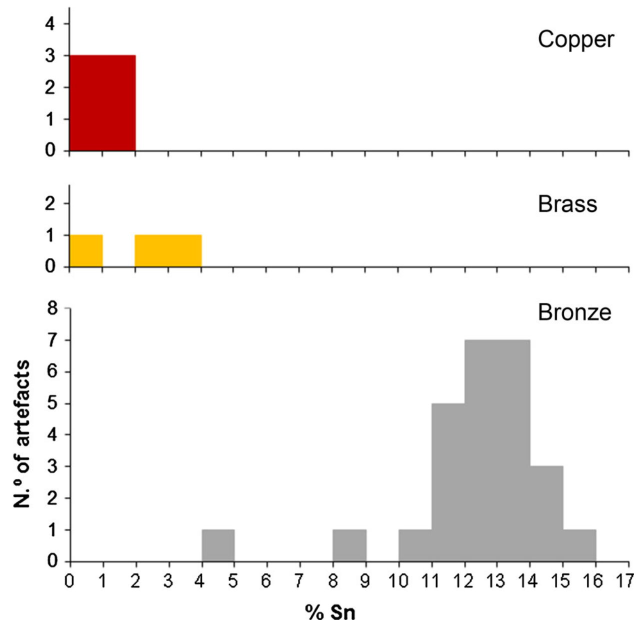

Fig. 6 Histograms of Sn content in the studied copper-based artefacts

of these artefacts being from a later chronology than LBA, as from Iron Age, Roman times, or even more modern.

The brass artefacts show very different compositions, with variable Zn, Sn and Pb contents, and the Fe content is always above 0.05 wt% (0.07–0.35 wt% Fe) evidencing relatively strong reducing conditions to obtain this type of alloy. Despite the differences in the compositions, the inclusions show some similarities, namely with Pb inclusions in the rings and ZnS inclusions in one ring and the capsule. The capsule also shows Pb inclusions associated with Bi and Bi inclusions. Interestingly, Bi inclusions were also detected in one of the copper rings (but without Pb), being the one that also had the higher Fe content (0.05 wt%).

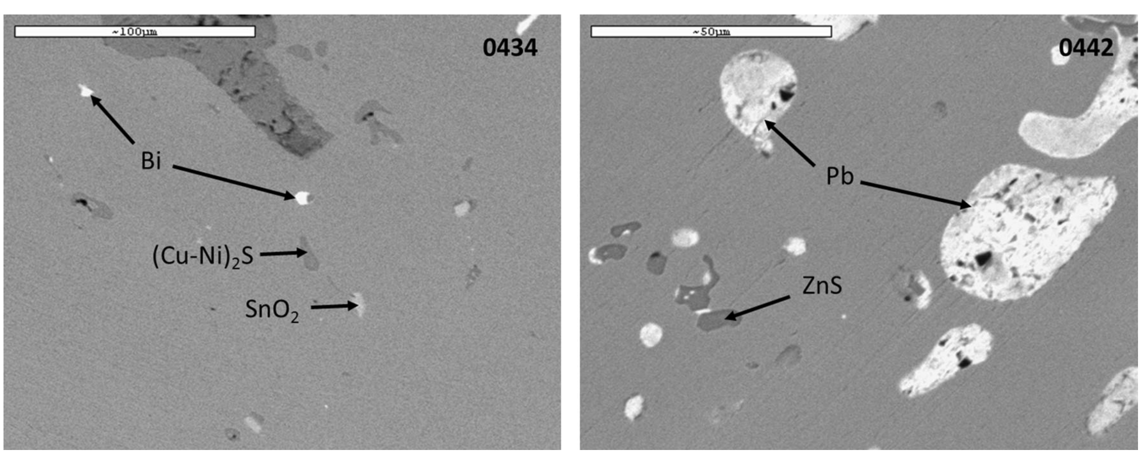

Fig. 5 SEM–BSE images with the identification of the Bi, $(Cu–Ni)S_2$ and SnO_2 inclusions in the copper ring 0434 and Pb and ZnS inclusions in the brass ring 0442

Comparing the composition of the MG brasses with the very few known early brasses [8], the rings which show variations in the Zn, Sn and Pb contents (and with Zn < 17 wt%), are the ones which could better fit an early brass production pattern. Nevertheless, their compositional variations could also be a result of recycling, as mixing brass with bronze or leaded bronze. Attending to the higher Zn content in the capsule and relatively low Sn and Pb contents, this alloy suggests that it was produced by cementation process. Thus, although no clear chronology can be suggested for the brass rings, the capsule appears to be from a period after the first century BC, as Roman or even more recent.

The analysis of the superficial and small-size material present in the capsule's outer surface revealed that it is made of a bronze alloy. Detailed SEM–EDS analysis showed a bronze with large amount of ($\alpha + \delta$) eutectoid, meaning that it was an alloy with relatively large amounts of Sn. Although the primary alpha phase is attacked by corrosion in most parts, unaltered areas showed that this phase also contained some Zn (Fig. 7). Semi-quantitative analysis made in some areas ($\sim$200 × 200 μm) showed Sn to be close to 34 wt% and clearly overestimated regarding the original non-altered metal alloy (preferential copper loss occurs in alpha phase due to corrosion [31]). Still, its microstructure points out to a bronze alloy with 20–30 wt% Sn.

This small bronze material could be the remains of a joining element, made to attach this object to another, as a dagger hilt, a necklace or a bracelet. This small capsule was likely an ornament. Given the small size of the bronze material on the surface and its high adherence to the base metal, it appears to be the remains of a soldering.

There are two types of soldering: soft soldering, which is the joining of metals by means of a low melting temperature metal or alloy, usually lead and/or tin, with the union being made without fusing the base metal or apparent alloying, and hard soldering, or brazing, which can occur at temperatures $\sim$550 °C up to 850 °C. The latter needs a skilful worker, and the solder is used to fill/bridge a very narrow space between base metal parts. Hard soldering results in very strong joints [32].

Since a Cu–Sn alloy has a relatively high melting temperature ($\sim$30 wt% Sn bronze has a liquidus temperature around 750 °C), it can be suggested that hard soldering that was used. This would also explain the presence of some Zn in the alpha phase (Fig. 7), which could be understood as partial melting of the base metal or as diffusion occurring during the process. Despite the scarce evidences of the use of Cu–Sn alloys as solders, Maryon [33] refers copper–tin as a hard solder used in Antiquity for copper, bronze or brass artefacts.

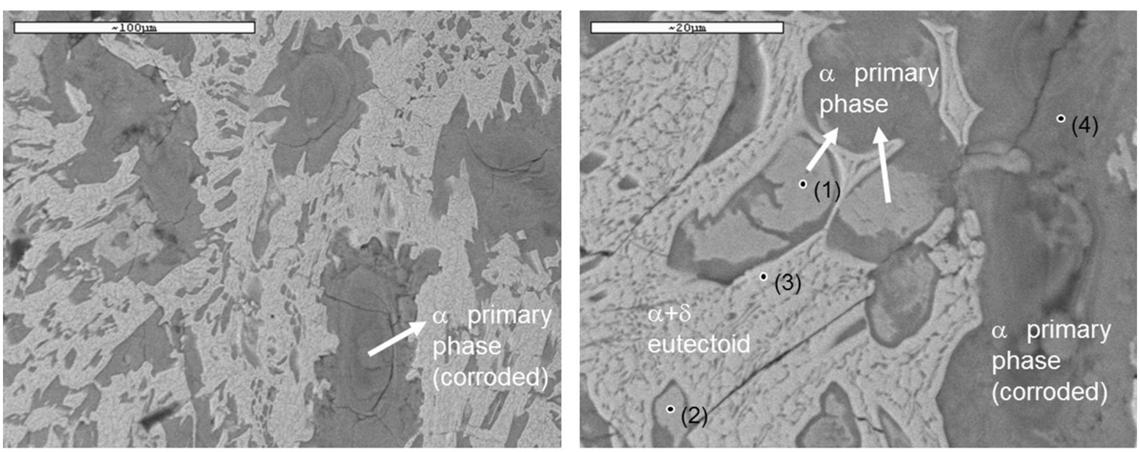

	Cu	Sn	Zn
(1) α primary phase	86.7	10.5	2.8
(2) α primary phase	85.5	11.4	3.1
(3) δ phase (with some influence from surrounding α phase)	71.8	28.2	n.d.
	CuO	SnO_2	ZnO
(4) corroded α phase	36.6	59.8	3.6

Fig. 7 Microstructure of the solder in the capsule 0457. At top SEM–BSE images and at bottom EDS analysis of alpha primary phase, unaltered and altered (corroded), and of delta phase in eutectoid (results in wt%, normalized)

3.3 Manufacturing techniques by optical microscopy

The optical microscope observations of the small prepared areas in the artefacts allowed for the observation of some common features within the metallic collection. The most regular characteristics found were equiaxial α grains with annealing twins. These appear after heating (recrystallization annealing) a cold worked metal (plastic deformation at low temperatures, generally by hammering) to recover its ductility. In some artefacts, the grains also showed slip bands, which are formed during cold deformation in the absence of a subsequent annealing. Some other artefacts exhibit a dendrite grain structure and/or cored grains, and thus remain with their as-cast microstructures.

In Fig. 8, the type of thermomechanical processing determined for the artefacts is presented regarding the type of metal and in the case of the rings also regarding their size. The majority of the artefacts suffered thermomechanical sequences (with annealing and deformation cycles). The bars and rings are those which presented a higher variety in the type of thermomechanical processing. This shows that some of them were either not fully finished artefacts or did not need any additional shaping or surface finishing after casting. In the case of the rings, the smaller ones tend to have been less processed than the larger ones. Also, it could be suggested that the brass rings were less processed than the copper or the bronze ones. Nevertheless, both brass rings have <2 cm in diameter, the three copper rings have ∼2 cm, while the larger rings (∼3 cm diameter) are all made of bronze, which would account for this differences.

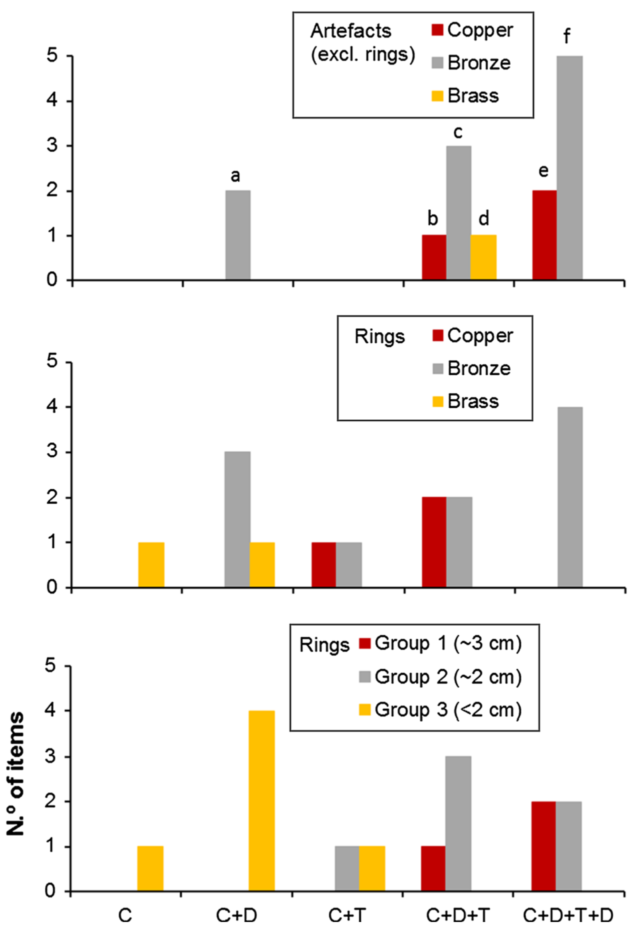

Fig. 8 Type of thermomechanical processing in the studied copper-based artefacts (C, Casting; D, Deformation/forging; T, heat treatment/annealing). In the artefacts (excl. rings): **a** pendant (pin) 0449, bar 0455; **b** sheet 0456; **c** button 0446, bar 0427, tranchet (blade) 0426; **d** capsule 0457; **e** bars 0453 and 0428; **f** daggers 0423, 0424, 0425, nail (pin) 0447, pendant (pin) 0448, bars 0450, 0451, 0452,0454

In some artefacts, it was possible to make observations in two or three different areas, to investigate the application of different thermomechanical processing in different parts of the objects. This was relevant in the daggers to investigate blade treatments and in objects that had parts with very different shapes, as the pendants or the nail.

In the daggers 0423 and 0424, different thermomechanical treatments between the blades, central rib and top of the handle were evident. In the dagger 0423, the central rib shows the presence of an as-cast microstructure, with many thin dendrites. The microstructure observed in the blade and in the top of the handle shows recrystallized grains, suggesting that after casting the object was only worked on the edges and not at the centre. This differential processing can be related to the final shaping and sharpening of the blade, since the blade needs to be thin and harder when meant for use. The microstructure of the dagger 0424 (Fig. 9) shows evidences of cycles of forging and annealing with different intensities at the centre and edge of the blade. The blade evidences a homogenized single α-phase with heavily deformed Cu_2S inclusions (long-shaped) and the centre of the blade shows a not totally homogenized alloy supported by the presence of some $(\alpha + \delta)$ eutectoid. At the top zone of the handle, it is possible to see the presence of slip bands which could have resulted from some deformation due to use, to break of the handle or related to some finishing operation to fit the hilt. Clearly, these daggers seem to have been finished objects with evidences of use.

The nail 0447 shows both parts of the artefact—the head and the pin—with microstructures composed by recrystallized grains with annealing twins, but the pin shows a high amount of slip bands. This suggests that after casting and annealing the object suffered a final cold deformation, which could be related to the shaping of the pin into a near-quadrangular cross section or to the process of fixing the nail to some base object. The pendant 0448 (Fig. 9) shows a dendritic microstructure homogenized by an annealing

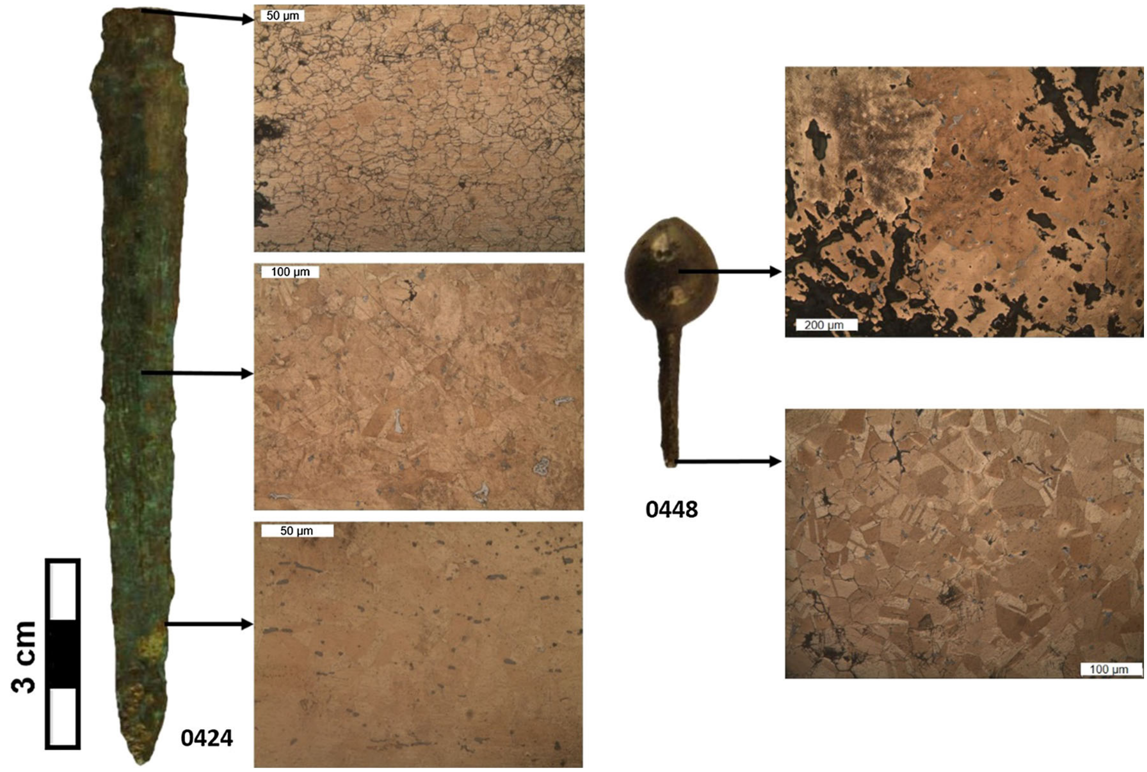

Fig. 9 Examples of different microstructures in the same object, at *left* on the dagger 0424 and at *right* on the pendant 2013-0448. All images were taken in BF and with etched surfaces

treatment at the head part, which was not sufficient to cause recrystallization of the grain structure. The microstructure of the pin part revealed recrystallized grains with annealing twins and some slip bands, evidencing a thermomechanical sequence of forging and annealing and possibly a final surface finishing. This microstructure suggests that this object was obtained in a mould, suffering some posterior thermomechanical treatments, mainly in the pin part. The pendant 0449 has an as-cast microstructure, with coarse dendrites and some superficial deformations (slip bands) in the head part, and the pin part has a dendritic structure with some evidence of superficial deformation. These microstructures suggest that this kind of object (pendant or hair pin) acquired its shape in a mould and suffered posterior minor works, either for shape corrections or for surface finishing.

4 Final discussion and conclusions

The study showed that the composition of the bronze artefacts are generally in agreement with the bronze metallurgical tradition undergoing in western Iberian Peninsula since the Late Bronze Age, with bronzes with 10–15 wt% Sn, low impurity patterns (namely < 0.05 wt%) and the presence Cu_2S inclusions. On the other hand, the copper artefacts which show low tin contents, metallic inclusions not previously observed in Bronze Age or earlier coppers (such as from the Chalcolithic period) in western Iberia, the presence of brass artefacts and eventually the low-tin bronze bar ($\sim$5 wt% Sn) seems to point out other metallurgical connections.

Despite the difficulty in attributing specific metallurgical contexts or connections to most artefacts, the presence of a diversity of metallic materials suggests that the Moinhos de Golas artefact collection results from the deposition of materials during different chronological moments and intentions. The first moment would have been in the Late Bronze Age, coeval with the ceramics that were collected at the site. This period is best represented by the three bronze daggers and the tranchet. Subsequently, during different moments, several materials could have been deposited or lost in the hill. If all the rings of copper, bronze and brass represent a coeval moment, this would have been, at the earliest, the Iron Age, assuming that Mediterranean influences reached northern Portugal at this time. However, independent moments of deposition and later periods cannot be neglected. The brass capsule has a composition which points out to the cupellation manufacturing process and thus to a period after the first century BC. This artefact in particular, could by itself, represent artefacts which were lost at the site in later moments since no ceramics from the Roman or later periods were found at the site (suggesting the absence of a permanent later occupation).

Finally, the present work shows the relevance of the use of complementary information obtained with an integrated analytical methodology in the study of archaeological metallic artefacts. The X-ray radiography was an important tool in terms of evaluating the presence of fractures and material heterogeneities, which provided information on ancient uses, technological fabrication and relevant information on the preservation state of the objects by mapping corrosion areas and fragilities. Many of these structural features, as fissures in wear/tension regions of daggers or the presence of a bronze solder in a brass capsule were not detected by naked eye, making this technique very relevant. The complementary use of elemental analysis by micro-EDXRF and SEM–EDS allowed to: determine the metal composition of the artefacts, showing that 73 % of the objects were made of bronze, 15 % of copper and 9 % of brass; determine the amount of different impurities relevant for the evaluation of metallurgical contexts (as Fe content); and also determine the type of inclusions in the metal matrices, which were different among the different alloys. Observations of the microstructure by optical microscopy allowed for the understanding of the manufacturing process of the artefacts, revealing that some objects were subjected to different types of thermomechanical processing in different parts of the artefact. This was the case of the daggers, which revealed much more processed blades than the central rib or handle parts.

Acknowledgments This work was funded by FEDER funds through the COMPETE 2020 Programme and National Funds through FCT—Fundação para a Ciência e Tecnologia under the project UID/CTM/50025/2013 to CENIMAT/I3N. C^2TN/IST authors gratefully acknowledge the FCT support through the UID/Multi/04349/2013 project. EF acknowledges FCT for the grant SFRH/BPD/97360/2013. JF acknowledge FCT for the grant SFRH/BD/65143/2009. Part of this project has been done in the framework of the FCT project ENARDAS (PTDC/HISARQ/112983/2009).

References

1. P.T. Craddock, *Early Metal Mining and Production* (The University Press, Cambridge, 1995)
2. M.L. Wayman, Mater. Charact. **45**, 259 (2000)
3. J. Fonte, A.M.S. Bettencourt, E. Figueiredo, Estudos do Quaternário **9**, 17 (2013)
4. R. Vilaça, Aspectos do povoamento da Beira Interior (Centro e Sul) nos Finais da Idade do Bronze (Trabalhos de Arqueologia 9—Instituto Português do Património Arquitectónico e Arqueológico, Lisboa, 1995)
5. A.M.S. Bettencourt, in *Existe um Idade do Bronze Atlântico?*, ed. by S.O. Jorge (Instituto Português de Arqueologia, Lisboa, 1998), p. 18
6. J. Castro Nunes, F. Bragança Gil, J.C. Senna-Martinez, F. Guerra, Artefacto metálico recolhido na Casa da Orca da Cunha Baica, concelho de Mangualde. Actas do I Colóquio Arqueológico de Viseu (Governo Civil do Distrito de Viseu, Viseu, 1989), p. 61
7. J. Loureiro, E. Figueiredo, R.J.C. Silva, M.F. Araújo, J. Fonte, A.M.S. Bettencourt, Estudos do Quaternário **11**, 59 (2014)
8. I. Montero-Ruíz, A. Perea, in *Metals and Mines: Studies in Archaeometallurgy*, ed. by S. La Niece, D. Hook, P. Craddock (Archetype Publications, London, 2007), p. 136
9. P. Valério, M.F. Araújo, A. Canha, Nucl. Instrum. Methods B **263**, 477 (2007)
10. E. Figueiredo, R.J.C. Silva, J.C. Senna-Martinez, M.F. Araújo, F.M. Braz Fernandes, L.J.I. Vaz, J. Archaeol. Sci. **37**, 1623 (2010)
11. E. Figueiredo, P. Valério, M.F. Araújo, R.J.C. Silva, A.M. Monge Soares, X-Ray Spectrom. **40**, 325 (2011)
12. E. Figueiredo, M.F. Araújo, R.J.C. Silva, R. Vilaça, Nucl. Instrum. Methods B **296**, 26 (2013)
13. N. Schiavon, A. Celauro, M. Manso, A. Brunetti, F. Susanna, Appl. Phys. A **113**, 865 (2013)
14. A. Celauro, N. Schiavon, A. Brunetti, L.-I. Mandredi, F. Susanna, A. Dekayir, V. Grazini, D. Pargny, D. Ferro, Appl. Phys. A **114**, 711 (2014)
15. P. Valério, R.J.C. Silva, A.M.M. Soares, M.F. Araújo, A.P. Gonçalves, R.M. Soares, Nucl. Instrum. Methods B **358**, 117 (2015)
16. P.T. Craddock, N.D. Meeks, Archaeometry **29**, 187 (1987)
17. C. Carvalho, F.S. Lemos, C. Meireles, Conjunto Mineiro Romano em Montalegre. Actas das XVI Jornadas sobre a Função Social do Museu (Câmara Municipal e Ecomuseu do Barroso, Montalegre, 2006), p. 147
18. C.P. Thornton, C.E. Ehlers, Inst. Archaeo-Metall. Stud. **23**, 3 (2003)
19. P.T. Craddock, in *2000 Years of Zinc and Brass*, ed. by P.T. Craddock (British Museum Occasional Paper 50, British Museum, London, 1990), p. 1
20. T. Rehren, M. Martinón-Torres, in *Archaeology, History and science: Integrating approaches to ancient materials*, ed. by M. Martinón-Torres, T. Rehren (Left Coast Press, Walnut Creek, 2008), p. 167
21. D. Dungworth, J. Archaeol. Sci. **24**, 901 (1997)
22. J. Bayley, in *2000 Years of Zinc and Brass*, ed. by P.T. Craddock (British Museum Occasional Paper 50, British Museum, London, 1990), p. 7
23. H. Bronk, S. Röhrs, A. Bjeoumikhov, N. Langhoff, J. Schmalz, R. Wedell, H.E. Gorny, A. Herold, U. Waldschläger, Fresenius J. Anal. Chem. **371**, 307 (2001)
24. E. Figueiredo, R.J.C. Silva, M.F. Araújo, J.C. Senna-Martinez, Microchim. Acta **168**, 283 (2010)
25. E. Figueiredo, R.J.C. Silva, M.F. Araújo, F.M.B. Fernandes, Microsc. Microanal. **19**, 1248 (2013)
26. D.A. Scott, *Metallography and Microstructure of Ancient and Historic Metals* (The Getty Conservation Institute & Archetype Books, Los Angeles, 1991), p. 69
27. P.C. Gutiérrez Neira, A. Zucchiatti, I. Montero-Ruiz, R. Vilaça, C. Bottanini, M. Gener, A. Climent-Font, Nucl. Instrum. Methods B **269**, 3082 (2011)
28. N. Kallithrakas-Kontos, A.A. Katsanos, J. Touratsoglu, Nucl. Instrum. Methods B **171**, 342 (2000)
29. A. Giumlia-Mair, E.J. Keall, A.N. Shugar, S. Stock, J. Archaeol. Sci. **29**, 195 (2002)
30. E. Figueiredo, J.C. Senna-Martinez, R.J.C. Silva, M.F. Araújo, Mater. Manuf. Process. **24**, 949 (2009)
31. L. Robbiola, J.M. Blengino, C. Fiaud, Corros. Sci. **12**, 2083 (1998)
32. H.H. Coghlan, *Notes on the Metallurgy of Copper and Bronze in the Old World* (The University Press, Oxford, 1975)
33. H. Maryon, Am. J. Archaeol. **53**, 93 (1949)